# ANALYSIS OF 4D SEISMIC TIME-SHIFT OVERBURDEN AND ITS RELATION WITH THE GEOMECHANICAL MODEL OF RESERVOIRS IN A CAMPOS BASIN FIELD

Carlos Américo R. Cardoso [ID][1], Fernando Sérgio de Moraes [ID][2], Kledson T. de Pereira e Lima [ID][3]

[1] Petrobras, Salvador, BA, Brazil

[2] Universidade Estadual do Norte Fluminense Darcy Ribeiro – Uenf, Macaé, RJ, Brazil

[3] Petrobras, Macaé, RJ, Brazil

*Corresponding author email: carlos_cardoso@petrobras.com.br

**ABSTRACT.** This paper seeks to interpret the 4D seismic time shifts in the overburden of a conventional turbidite sandstone reservoir in the Campos Basin and to calculate an empirical factor of sensitivity between these 4D data and the geomechanical deformations. Gaining information on how the production of the reservoir affects the surrounding rocks is of great interest for the management of oil fields, with impacts ranging from optimization of production to the safety of operations and workers. The study of time-shift anomalies is common in chalk fields and unconventional fields of high temperature or pressure. We used two techniques for time-shift calculations: cross-correlation and DTW, as well as structural attributes that are calculated to assist in interpretations. Then, we estimated the sensitivity factor, which allows the construction of synthetic 4D time shifts from the deformations simulated by the geomechanical model. In most of the field regions there was agreement between simulated deformations and 4D anomalies, showing that it is possible to extract useful information for reservoir management. The estimate of the sensitivity factor indicates that the overburden studied is sensitive to deformations in the rocks, allowing the small deformations to be detected by the given 4D seismic.

**Keywords:** R Factor; time strain; time-lapse; turbidite; deformations.

## INTRODUCTION

The time-lapse seismic method is now extensively used to aid the development of oil reservoirs, as the data differencing is able to highlight areas where reservoir properties have changed due to reservoir production during the time interval between the two seismic data acquisitions. Reservoir production generates many changes, affecting reservoir elastic properties, the distribution of geomechanical stress and the seismic (propagating) wavelet. In first order, observed time-lapse seismic data volumes respond to these effects in terms of seismic amplitude and traveltime differences. Amplitude changes of seismic reflections at reservoir interfaces are related to changes in the reflection coefficient, accompanying the changes in reservoir elastic properties in the reservoir layer due to production. Traveltime differences can be explained by a combination of changes in velocity, layer thickness (due to compaction or extension) and wavelet phase. Time-shift estimation and correction must precede the amplitude differencing to properly align seismic events. In this way, the amplitude will correspond to the changes in reflection coefficients at a given interface. Traditionally, time-shift data have been solely estimated with the purpose of obtaining the correct amplitude difference volume.

All producing reservoirs undergoing pressure drop are expected to compact to some degree. The strength of the reservoir compaction depends on the degree of the reservoir depletion, reservoir strength and stress conditioning by surrounding rocks. The redistribution of stress in the overburden as a consequence of production effects in the reservoir layer causes small deformations and changes in the seismic velocities, which are generally detectable by the seismic reflection method. Since the thickness of the overburden usually varies

from one to several kilometers, even small changes of velocity, less than one percent, can accumulate to yield detectable time shifts near the top of the reservoir (Røste et al., 2015). Stress changes in overburden rocks can lead to shifts, fractures and reactivation of faults, ranging from less critical stress changes, inducing small-scale vertical displacements (millimeters to centimeters) to more severe stress changes, inducing fractures and reactivation (Barkved et al., 2003). Examples in the North Sea, in some chalk-type reservoirs, can compress more than ten meters during field production, inducing significant changes with great impact on well management (MacBeth et al., 2018).

Geomechanical simulations may explain changes in seismic wave transit time in 4D seismic data due to the effects of reservoir production (Landrø and Stammeijer, 2004; Hatchell et al., 2005a; Herwanger, J., Palmer, E., and Schiøtt, C. R., 2007). Other effects that may be related to 4D time shift, such as subsidence (Fiore et al., 2014) and variation in pore pressure in layers above the reservoir (Garcia, A. and MacBeth, C., 2013), are related to geomechanical effects. In addition, these effects may show some significant complexities depending on the geometry (Dussault et al., 2007) or overburden lithology (Wong and MacBeth, 2016).

Detailed analysis of the time shift in the overburden region is highly useful for field management. Considering that the seismic monitoring of the reservoir is normally used to map the remaining reserves, the overburden study can help avoid situations of risk to workers' health, safety and environmental tragedies, as well as drilling problems. Leakage of hydrocarbons, other wastes in seawater, or oil spills in deep waters represent some cases with high potential for environmental and economic impact.

For fields with normal pressure and temperature sandstone reservoirs, overburden time shifts are less expected as reservoir rocks when comparing with chalk-type reservoirs. For this reason, time shifts in conventional sandstone reservoirs are of little interest. Among the examples found in the literature, the interpretation of the Snorre, Heidrun and Statfjord sandstone fields by Røste and Ke (2017) shows the potential of this analysis in such reservoirs. Although sandstone reservoir compacting is generally small (centimeters) and often is not a problem for well drilling, it is important to obtain and understand all time shifts in the overburden to separate pressure effects from saturation effects within the reservoir and discriminate the geomechanical effects of other phenomena.

The objective of this paper is to describe and understand the relationship between 4D seismic and geomechanics in the overburden and to explain the time shifts observed in the overburden of a turbidite field in the Campos Basin, performing a flow of steps to estimate an R Factor (empirical factor of sensitivity of the rock and relation to deformation) that relates vertical deformations estimated by the geomechanical model and variations in the seismic velocities, thus allowing to model the time shift from a geomechanical model and confronting it with real time shifts. Therefore, we seek to evaluate the geomechanical model of the field and facilitate the understanding of the relations of future events resulting from the production observed in 4D seismic. A good correlation between time shifts modeled and observed in some areas of the field indicates that the signal in the overburden is real and is caused by geomechanical changes, while a weak correspondence indicates that the observed time shifts are related to non-geomechanical effects. The analysis is restricted to overburden and mainly the geomechanical and 4D seismic relation. Non-geomechanical explanations of time shifts are quoted but are not described in detail.

## CAMPOS BASIN FIELD

The field studied in this paper has a turbiditic reservoir of the Carapebus Formation, formed in the Paleogene period, of Oligocene age, at a depth of about 2,600 meters. The reservoir is formed by sandstones with excellent permoporous characteristics, high productivity and API oil between 17-24 degrees API. The primary mechanism of production is the gas in solution, with the use of water injection as a secondary oil recovery mechanism. According to Mohriak et al. (2008), two distinct structural styles coexist in the basin. The first one, circumscribed to the deposits of the rift phase, is characterized by a system of steep normal faults involving the basement, with preferred direction NE / SW. The second tectonic domain is related to the salt movement and begins after the formation of a carbonate platform in the Lower Albian. Despite the division, some of the faults that affect salt and overlapping rocks appear to be related to the basement structures, such as reactivated transfer zones. As described by Demercian et al. (1993), the Campos Basin can be divided into three main domains, with the pattern of structures related to the tectonics. The field of study of this paper is located in the first domain, denominated extensional

halokinetic domain, that has a width of 100 to 200 km, depth of sea water up to 1400 m and comprises structures related to the horizontal extension dive below. It is characterized by salt rollers under high blocks of growth cracking; salt walls with triangular cross-section, above which normal conjugated faults are common; anticlinal "tortoise shells"; and salt scars. Figure 1 shows a dip section of the area where it is possible to see a diapir of salt in the western part of the field, forming an extensional structure in graben format controlled by a listric fault growth. There is also in the eastern part of the field a similar structure with an antithetic fault that conditions the field. The two structured regions present themselves as a probable migration route. The structural pattern in the western part indicates that the salt-depleted stratum of the mother layer underwent a small collapse, also causing the formation of a graben. The continuous reactivation of the faults and the syndepositional process of the movement of the diapir very probably caused the deposition of the turbidite body under study, being largely responsible for the accumulation of hydrocarbons in the reservoir.

The seismic data used in this paper were acquired in the years of 1997, 2005 and 2010. The processing was done specifically for the 4D analysis, designed to highlight the differences caused by the effects of field production.

# TIME-SHIFT 4D AND GEOMECHANICS IN OVERBURDEN

The geomechanics of reservoirs seeks to understand, based on the mechanical theory of rocks and encompassing the hydromechanical behavior of natural fractures, the propagation of hydraulic fractures, solid production, stability and well integrity. Studies of geomechanics of reservoirs are characterized by multidisciplinarity, since they depend on the knowledge of reservoir engineering, structural geology, geophysics, rock mechanics and well engineering. Therefore, the geomechanical model contemplates information that is commonly raised by professionals of different formations acting in different areas. Increasingly, it is necessary to develop these studies to support decisions related to the strategy of production of oil reservoirs. Among the main objectives of a study of geomechanics, there are optimization of production and mitigation of environmental risks.

# Geomechanical Modeling

The objective of the geomechanical model is to estimate the displacements, deformations and changes of the state of tensions that occur in and around the reservoir. These changes are usually caused by changes in pore pressure as the reservoir is produced. The drop in pore pressure leads to changes in stress, not only in effective stress, but also in total stress. These stress changes not only control compaction and subsidence but can also lead to changes in the reservoir flow performance. The permeability may change and the flow preference directions may also be changed. In some cases, stress changes in and around the reservoir cause seismicity during reservoir depletion. The dynamic nature of oil reservoirs allows the observation of several phenomena that assist in the management of reserves. When oil or gas is produced from a reservoir, the pressure of the fluid generally decreases. Reducing pore pressure in the reservoir rock will increase effective stress and, as such, will cause the rock itself to shrink and will compact the reservoir. The compaction of the reservoir can then, in turn, cause subsidence in the area. The first report on subsidence is from the Goose Creek field, Texas, in 1918 (Pratt and Johnson, 1926). Later, in the 1920s, another well-known case is the Wilmington field in Long Beach, California, where a subsidence of nearly nine meters was detected. More recent examples are the Ekofisk and Valhall reservoirs in the Norwegian North Sea region (Zoback and Zinke, 2002).

As discussed by Fjaer et al. (2004), to calculate the compaction of a reservoir in a simple and basic case, we assume the linear poroelasticity and consider a homogeneous reservoir made up of isotropic rock. The deformation of the reservoir can be expressed by Hooke's law in terms of changes in the effective stress, using the initial stress state, that is, the start of production as a reference. Considering a two-dimensional reservoir model of thickness h, Young's modulus E, Poisson ratio v, strain ε, effective stress σ and starting from Hooke's law, we have:

$$E\varepsilon_{xx} = \Delta\sigma'_{xx} - \nu\left(\Delta\sigma'_{yy} + \Delta\sigma'_{zz}\right) \qquad (1)$$

$$E\varepsilon_{yy} = \Delta\sigma_{yy}' - \nu\left(\Delta\sigma_{xx}' + \Delta\sigma_{zz}'\right) \qquad (2)$$

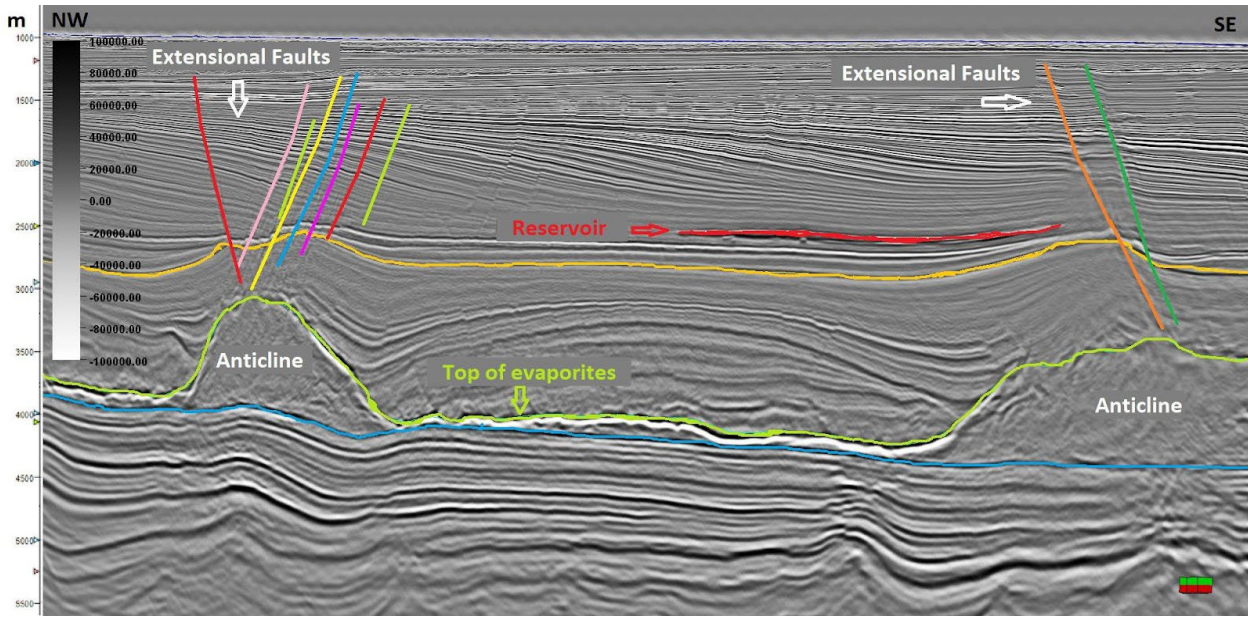$$E\varepsilon_{zz} = \Delta\sigma_{zz}' - \nu\left(\Delta\sigma_{yy}' + \Delta\sigma_{xx}'\right) \qquad (3)$$

Figure 1: Seismic section with regional landmarks of the field of study in the Campos Basin.

The variation in the thickness of the reservoir, Δh, is given by the vertical stress zz and the thickness of the reservoir h, that is:

$$\Delta h = -\varepsilon_{zz} h \qquad (4)$$

The compaction of the reservoir corresponds to a negative Δh. Since the lateral extension of a reservoir is usually much larger than its thickness, it is reasonable, as a first hypothesis, to neglect the lateral deformations considering only the uniaxial deformation in the vertical direction; thus:

$$\varepsilon_{xx} = \varepsilon_{yy} = 0 \qquad (5)$$

To compute compaction, we need to know how tensions evolve. For uniaxial vertical compaction during depletion, the effective horizontal stress needs to increase. This way:

$$\Delta \sigma_{xx}' = \Delta \sigma_{yy}' = \frac{\nu}{1-\nu} \Delta \sigma_{zz}' \qquad (6)$$

We assume that the total vertical stress acting on the reservoir remains constant during the production, which means that the entire overburden weight is detected by the reservoir whenever the pore pressure is reduced (zz = 0). Thus, the arc of stress that would support part of the depletion is neglected.

$$\Delta \sigma_{zz}' = \Delta \sigma_{zz} - \alpha \Delta p = -\alpha \Delta p \qquad (7)$$

where α is the pore-elastic coefficient of Biot, given by:

$$\alpha = 1 - \frac{K_{fr}}{K_s} \qquad (8)$$

where $K_{fr}$ is the volumetric module of the complete rock and Ks is the Bulk module of the rock matrix. By rearranging the equations presented so far, we arrive at the following vertical deformation formula:

$$-\varepsilon_{zz} = \frac{\Delta h}{h} = \frac{1}{E} \frac{(1+\nu)(1-2\nu)}{1-\nu} \alpha \Delta p \qquad (9)$$

Thus, since the elastic properties E, v, the pore-elastic coefficient α and the thickness of the reservoir h are known, we can define a compression coefficient or uniaxial compressibility Cm, such as:

$$\frac{\Delta h}{h} = Cm\alpha\Delta p \qquad (10)$$

$$Cm = \frac{1}{E} \frac{(1+\nu)(1-2\nu)}{1-\nu} \qquad (11)$$

## Time shifts in 4D Seismic

The difference in transit time between traces of two 4D, base and monitor seismic data, processed at the same velocity field, is the time-shift function. As the traces of two acquisitions in the same area are very similar, the small difference between them is this function, given by:

$$X_{base}(t) \approx X_{monitor}(t + \tau(t)) \qquad (12)$$

Being τ (t) the time-shift function.

As discussed by Landrø and Stammeijer (2004) and Hatchell and Bourne (2005a), considering a thin horizontal layer with thickness and velocity of the compressional wave v, having t as the time of compression from the compression wave to normal incidence, the changes in transit time caused by small variations in the thickness and velocity in the layers, $\Delta z/z \lll 1$ and $\Delta v/v \lll 1$,, can be expressed by:

$$dt = \left(\frac{\partial t}{\partial z}\right)_v dz + \left(\frac{\partial t}{\partial v}\right)_z dv \qquad (13)$$

Calculating the partial derivatives for t = z / v, we have:

$$\frac{dt}{t} = \frac{dz}{z} - \frac{dv}{v} \qquad (14)$$

Attempts to estimate time shifts may so far be divided into three major categories: manual, window correlation, and error minimization. The manual includes manual event picking and automated picking, such as maximum amplitude picking. These approaches are reasonably robust and accurate (Landrø, 2001), but require significant human interaction, which makes them costly and time-consuming. Estimates of this kind hinder other analyzes such as the time-shift derivation.

Window approaches, most notably the window cross-correlation approach, are more or less automated. This approach assumes that the signals to be compared are locally similar and that the differences can be explained by translation along the time axis. With rapidly varying time shifts, this assumption involves ever narrower windows and, consequently, less robustness. On the other hand, if wide windows are used to ensure stability, the result is imprecise estimates at the position of the time shifts along traces. The error minimization approaches are fully automated and seek to calculate the errors between two time series in an optimization process, so that the proposed correction is the best path between the series. In this paper, cross-correlation techniques were used with two window sizes, one larger and one smaller, seeking the balance between performance and stability. Another automated technique, known as Dynamic Time Warping, was also used. These techniques are described by Hale (2013).

## Time strain

Time shifts are cumulative, so they can appear at reservoir level and were caused in overburden regions. Thus, the correct location of velocity variations can be obtained by the time-shift derivation, known in the literature as time strain, and expressed by Røste and Ke (2017) as:

$$\frac{\Delta v}{v} = -\frac{d(\Delta t)}{dt} \qquad (15)$$

This equation is valid when we assume that the time shifts are caused mainly by the velocity variation, that is, that the displacements caused in the layers due to the deformation are negligible. The time-strain volume is calculated directly from the volume of time shifts and has the advantage of solving subsidence effects and highlighting locations with large velocity variations due to unexpected effects. In this paper the volume of time strain is of extreme importance to make the connection between 4D seismic and geomechanical reservoirs.

## R Factor

As proposed by Hatchell and Bourne (2005a) and almost simultaneously by Røste et al. (2005), for the normal incidence of the wave, there is a linear relation between the variation of the deformation (compression or dilation) and the variation of the velocity of propagation, that represents the connection between the 4D seismic and the geomechanics, being able to be represented by a factor "R". Normally, the more compacting the rock suffers, the greater the velocity of propagation of the wave in that medium tends to be.

$$\frac{\Delta v}{v} = -R\frac{\Delta z}{z} \qquad (16)$$

R is an empirical parameter of rock sensitivity to deformation. In overburden, it depends mainly on the initial state of stress and the lithological composition. Thus, knowing that in geomechanics the $\Delta z / z$ is the equivalent of the vertical strain tensor, zz, we have:

$$\frac{\Delta v}{v} = -R\varepsilon_{zz} \qquad (17)$$

Replacing in $\Delta t / t$:

$$\frac{\Delta t}{t} = (1 + R)\varepsilon_{zz} \qquad (18)$$

Positive values of R indicate that a positive deformation (dilatation) causes a decrease in velocity. MacBeth et al. (2018) cite some important observations about the results of the R Factor estimates of several fields, considering the geomechanical effect the main reason for the appearance of time shifts, relating them through the geomechanical modeling of reservoirs and time shifts extracted directly from seismic 4D, among them:

a) Decreases in seismic propagation velocity due to layer expansion are more commonly observed in the overburden and in the reservoir than an increase in velocity caused by compaction in the same layers, whereas in the geomechanical simulation this asymmetry does not occur;

b) Increases in seismic velocity are rarely caused by increased stress above injectors. The velocity increase is expected to occur above the injection of water or gas injectors that inflate the pressure in the reservoir, which is rarely observed;

c) Geomechanical effects induced seismic velocities to relate to whole rock volumes and spread through many types of lithology. Time strains appear diffused and distributed in large volumes of rocks in subsurface and, therefore, are not confined to discrete interfaces. In fact, they are observations that show long wavelengths and seem to imitate the character of the geomechanical deformation caused by effects of production;

d) Observations exhibit hysteresis. Already known in geomechanics, it is also possible to be noticed in the behavior of the variation of the seismic velocities in the overburden.

MacBeth et al. (2018) still show through laboratory experiments that for a more complete analysis of the estimates of the values of the R Factor, volumetric deformation must be taken into account, especially for estimates in the rocks of the reservoir, since in this region the deformations are more intense in all directions.

## METHODS

The main cause of anomalies of time shifts in the overburden is the variation of the pressure in the reservoir. As previously discussed, the pressure variation causes geomechanical effects that deform the rocks of the reservoir and, consequently, the rocks around it. Based on this information, we will first analyze the pressure variation in the field of study between the periods of the 1997, 2005 and 2010 seismic surveys (Figure 2). The delta pressure data are provided by the flow simulator and aim to adjust the field pressure from measurement pressure during the implementation of wells and the mass balance in the reservoir, honoring the production history. These data are of extreme importance for geomechanical simulation and cover the entire field life from the first oil to the end of production.

The pressure variation map between 1997 and 2005 can be divided into three groups. To the north of the field, we have a depletion, to the center, an overpressure and, to the south, we have a drop of pressure again, only that with greater intensity than the anomaly of the north region. There is a lithological barrier between the central zone and the zone to the south that does not prevent the hydraulic connection between the zones but does not behave as a full connection. Between the north and central zones, there is no defined lithological barrier, but there was a management of the injection wells and producers that resulted in a very positive balance for the injection in the central zone due to low production of oil in this region. The pressure variation map between 2005 and 2010 can be divided into two groups with small variations. To the north of the field, we have an overpressure, to the center and to the south, a pressure drop. At that date, due to the small pressure variation, both upwards and downwards, no large geomechanical deformations or significant time-shift values were expected in much of the reservoir. The pressure variation map between 1997 and 2010, the cumulative two variations noted above, can also be divided into three groups, similar to those in the 1997-2005 range. To the north of the field, we have a depletion, an overpressure
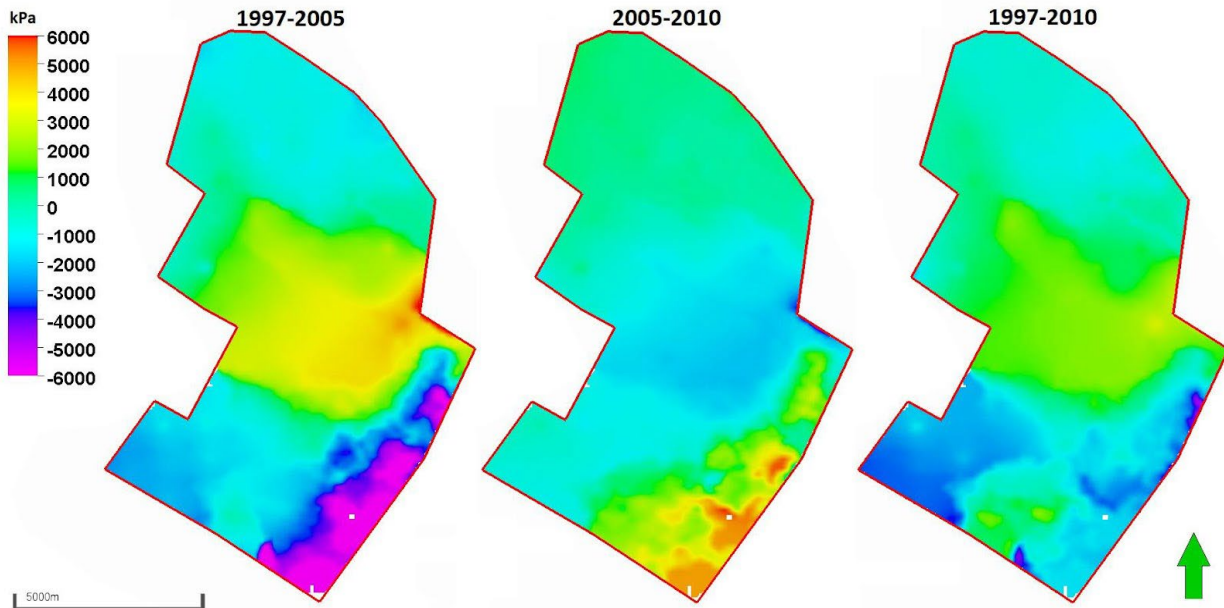
Figure 2: Pressure variation in the reservoir on 4D dates.

in the center, attenuated by the depletion between 2005 and 2010 and, to the south, we have a drop in pressure. At that date, as in the period between 1997 and 2005, the southern region of the field presents greater chances than in the period between 2005 and 2010 to present significant time-shift anomalies in the 4D seismic.

In practice, any pressure variation causes deformations in the rocks of the reservoir; however, to have sufficient deformation to cause variations in the velocity of propagation of the seismic wave, it is necessary that these small deformations, besides displacing the position of the rock, be sufficient to change the stress field. The rocks in the reservoir under study have good permoporous characteristics and deform relatively easily because they are unconsolidated sands.

## 4D amplitudes

In order to compare 4D amplitude properly, the correction of the time shifts is necessary. The process of correcting differences in the positions of events between given monitor and base is called warping. In the monitor volumes supplied for the accomplishment of this study, the correction was applied so that we can calculate the volume amplitude differences directly from these corrected data. With the calculated volumes, it was possible to extract the difference amplitudes (Figure 3) between the data to obtain the map of the 4D anomaly.

The calculated maps have a geometric characteristic that mimics the direction of acquisition,

showing that the results are partially hampered by the noise associated with acquisition or processing that could not remove these undesired effects, even though the anomalies corroborate in large part with the data of the field production. Between 1997 and 2005, the north and center regions of the difference amplitude map in the reservoir show an increase in impedance, mainly associated with the arrival of water in the layers closest to the top. In the southern region, some strong impedance drop anomalies appear, which are most likely associated with the formation of a gas cap. Between 2005 and 2010, the anomalies are weaker and of less occurrence, complicating the identification of a behavior by zones. The total period, from 1997 to 2010, reinforces the characteristics seen between 1997 and 2005, only highlighting some points with greater intensity.

## Deformations and displacements

The vertical strain tensor, zz, is a product of the geomechanical simulation and is represented by the volume of deformations in the z-direction. The sum of these deformations layer by layer is the displacement volume, which measures the total displacement of the layer relative to a datum. As the result of the simulation is given in steps, the measurements were calculated only in the periods of the 4D surveys. For a corresponding analysis, the displacement must be correlated to the time shift, which represents the sum of the variations of seismic velocities. Deformations must be correlated to time strains.
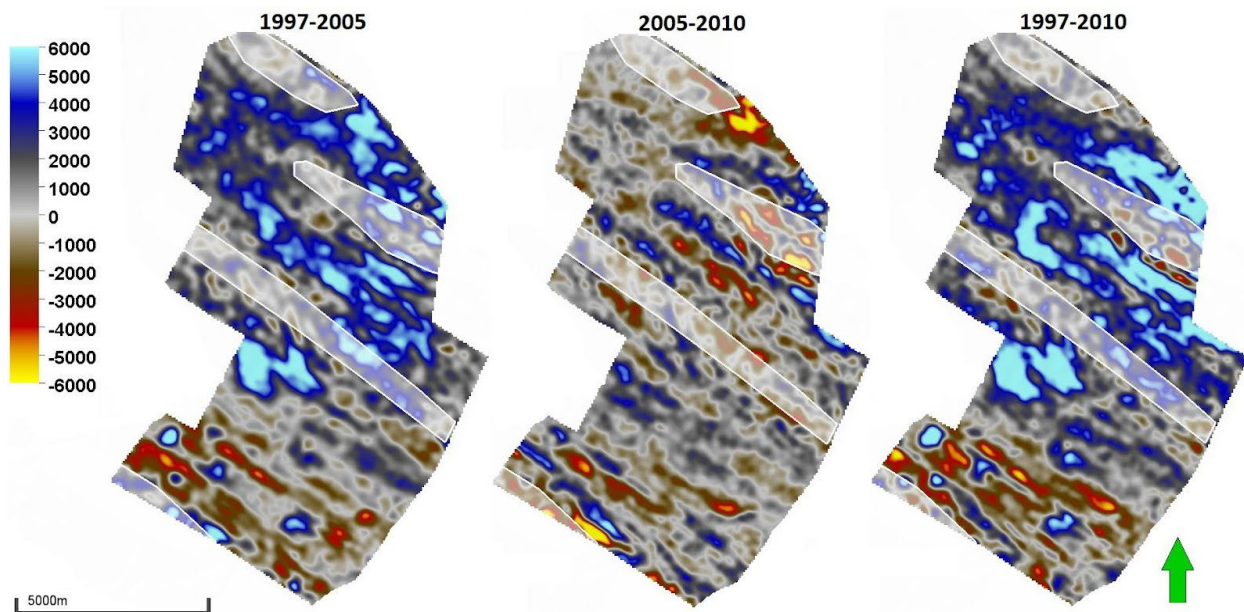
Figure 3: Amplitude difference in 4D dates at the top of the reservoir. The white zones represent seismic lack of coverage.

## Extraction of time shifts

Several time-shift volumes were calculated by varying the available parameters. The common parameter between the cross-correlation and the DTW is the maximum shift, or maximum time shift, defined here for 20 ms. The definition of the maximum shift value depends on the intensity of the expected velocity variations, which can be between 10 and 50 ms. For conventional sandstones, low time-shift values are expected between 2 and 10 ms (MacBeth et al., 2018). Thus, the choice of 20 ms for the maximum encompasses the expected consistent anomalies well and prevents the techniques from erroneously correlating events too much.

For the cross-correlation calculation there is one more parameter to be defined, the correlation window in number of samples or milliseconds. As previously quoted, a large window improves the stability of the process; however, it ends up considerably shifting the time shifts from their actual positions in depth. From this, the windows of 140 ms and 200 ms were applied. The results are in accordance with the expectation, as shown in Figure 4. The window 140 is slightly noisier than the window 200, but better positions the time shifts of their real positions.

For interpretative analyzes, the data with window 140 were chosen. The choice of the window for the calculated volume depends on the interpreter and the characteristics of the seismic data, and there are no pre-defined ideal values in the literature. The parameters

available for the DTW calculation are the maximum shift and the Gaussian smoothing coefficient; the lower the coefficient, the smoother the data become. Among the tests performed, two examples are presented in Figure 4. Smoothing data 10 result in amplitudes with smoother breaks when compared to smoothing 8. Both have better location of anomalies on the vertical axis than those calculated by cross-correlation. For interpretive purposes, the smoothing data 8 were chosen; similarly to the decision in the correlation window, it is the choice of the interpreter. All the time-shift images that are presented in this paper are with scale ranging from -6 to 6 ms, with the blue color representing the positive values and consequently representing a decrease in the seismic velocity of the monitor in relation to the base.

## Statistical Estimation of R Factor

The observed data matrix is represented by the actual time shift. The calculated matrix is represented by the integration of the matrix column resulting from the multiplication of an arbitrary R factor by the strain matrix of zz. In the search for an R Factor closer to the real, an objective function was used to calculate the errors between the calculated and observed matrix. The minimum error was found by the least squares technique.

Describing the steps:

Function that generates the synthetic time shift from the synthetic time strain, given by Hatchell and Bourne (2005b):
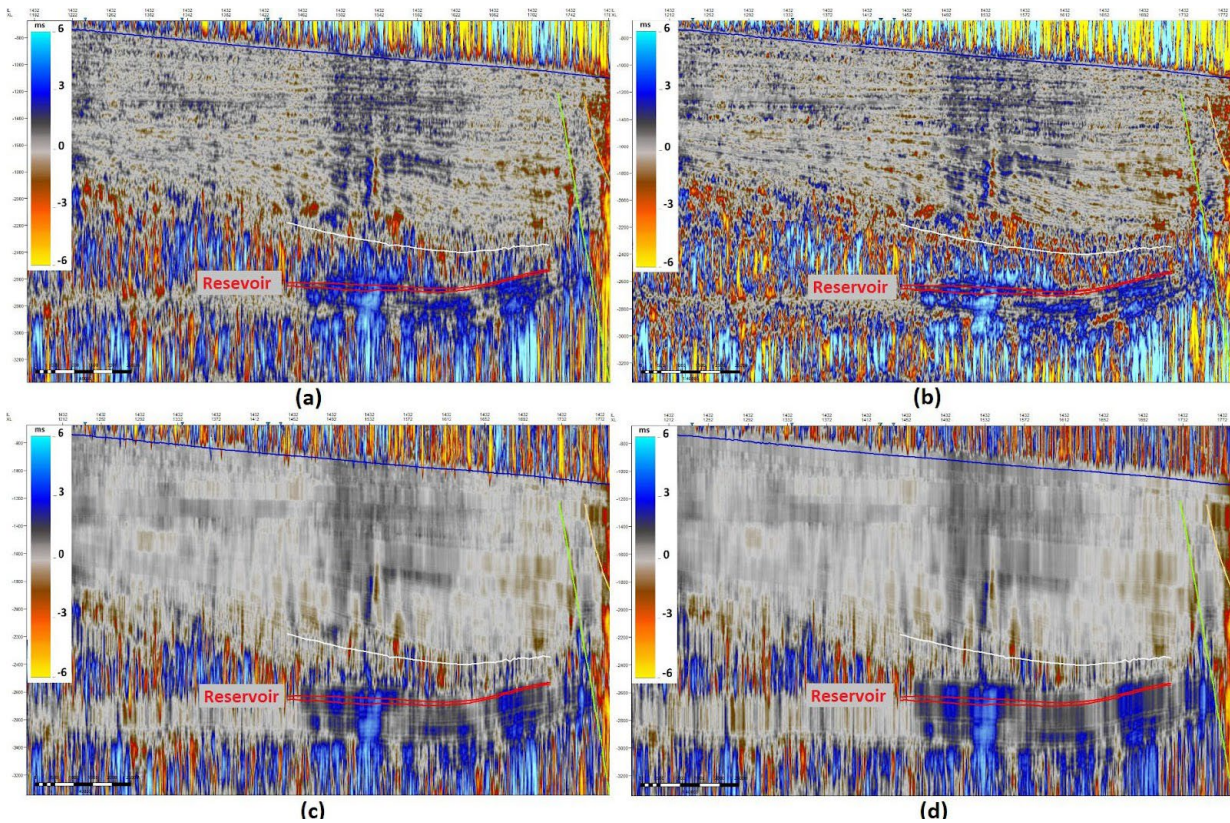
Figure 4: The time shift calculated by the DTW technique, (a) with smoothing 8 and (b) with smoothing 10. The time shift calculated by the cross-correlation technique, (c) with window 140 and (d) with window 200.

$$(\Delta t)_{calc} = \int_0^z (1+R)\frac{\varepsilon_{zz}}{v} dz \qquad (19)$$

Objective function with size MxN elements:

$$M_{dif} = (\Delta t)_{calc} - (\Delta t)_{obs} \qquad (20)$$

The value of the error associated with the arbitrated R is given by:

$$E_{rr} = \sum_{k=1}^{MxN} (e_{i,j})^2 \qquad (21)$$

At the end of the process, the R Factor with the lowest associated error is chosen to calculate the synthetic time shift. Figure 5 shows a region chosen in a region of the field that there is a great correlation between the geomechanical simulation and the 4D anomaly.

In Figure 6, there is the result of the estimate following the steps described above, with the result found R = 1300. This value is discussed calmly in the section of discussion and the synthetic time shift generated with this factor is compared to the real.

## RESULTS

In order to show a significant part of the field of study, representative sections (Figure 7) of the area covering most of the regions of interest were chosen, focusing mainly on the lower noise zones and the main zones of deformation. The dip A section is in the southern region of the field where depletion occurs in much of the period between 1997 and 2010, showing a slight overpressure between 2005 and 2010 in part of the area. The southern region presents the highest correlation between time-shift anomalies and simulated geomechanical displacements.

Considering approximately that the expected movements are between 1 and 5 cm, it is unlikely that these small movements in kilometers of overburden can change the seismic velocities to the point of being detected; however, in that region, the correlation is indicative that the 4D anomalies are caused by the geomechanical effect and not for other reasons. Figure 8 shows the result of the geomechanical simulations of the same section next to the time shifts calculated by the DTW technique. As previously explained, depletion anomalies are much more detected than overpressure
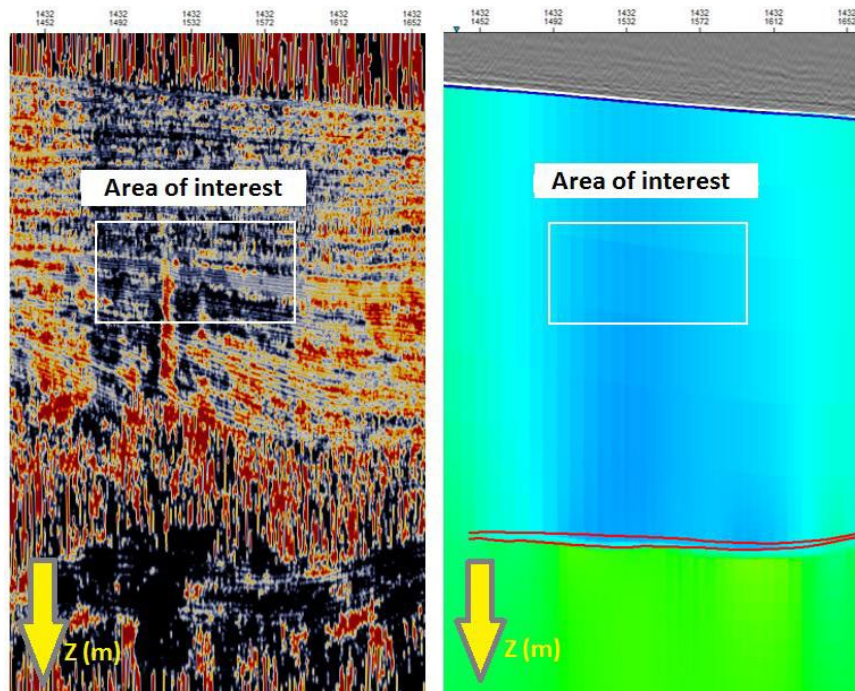
Figure 5: Region selected for estimate R. The right picture demonstrates the simulated displacement between 1997 and 2005, and the left picture shows the time shift calculated by the DTW technique between 1997 and 2005.
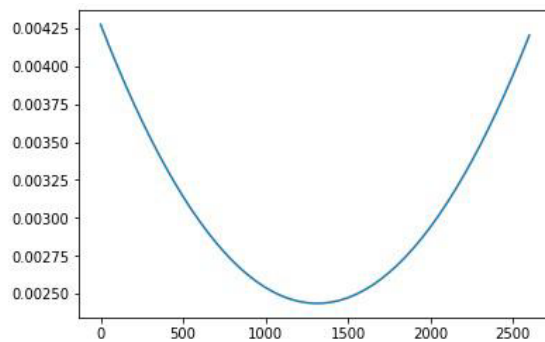


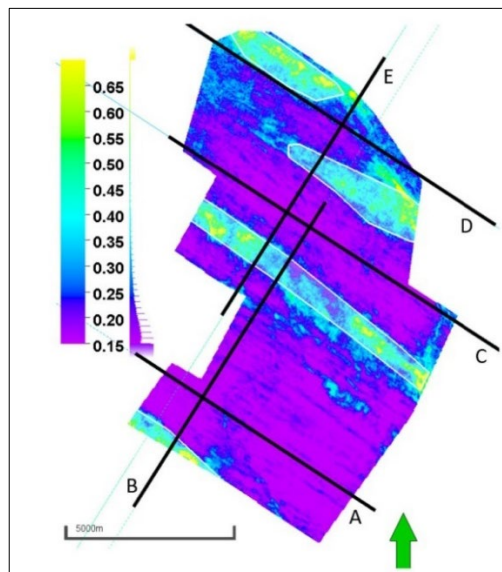Figure 6: R Factor = 1300 estimated by the least error associated.



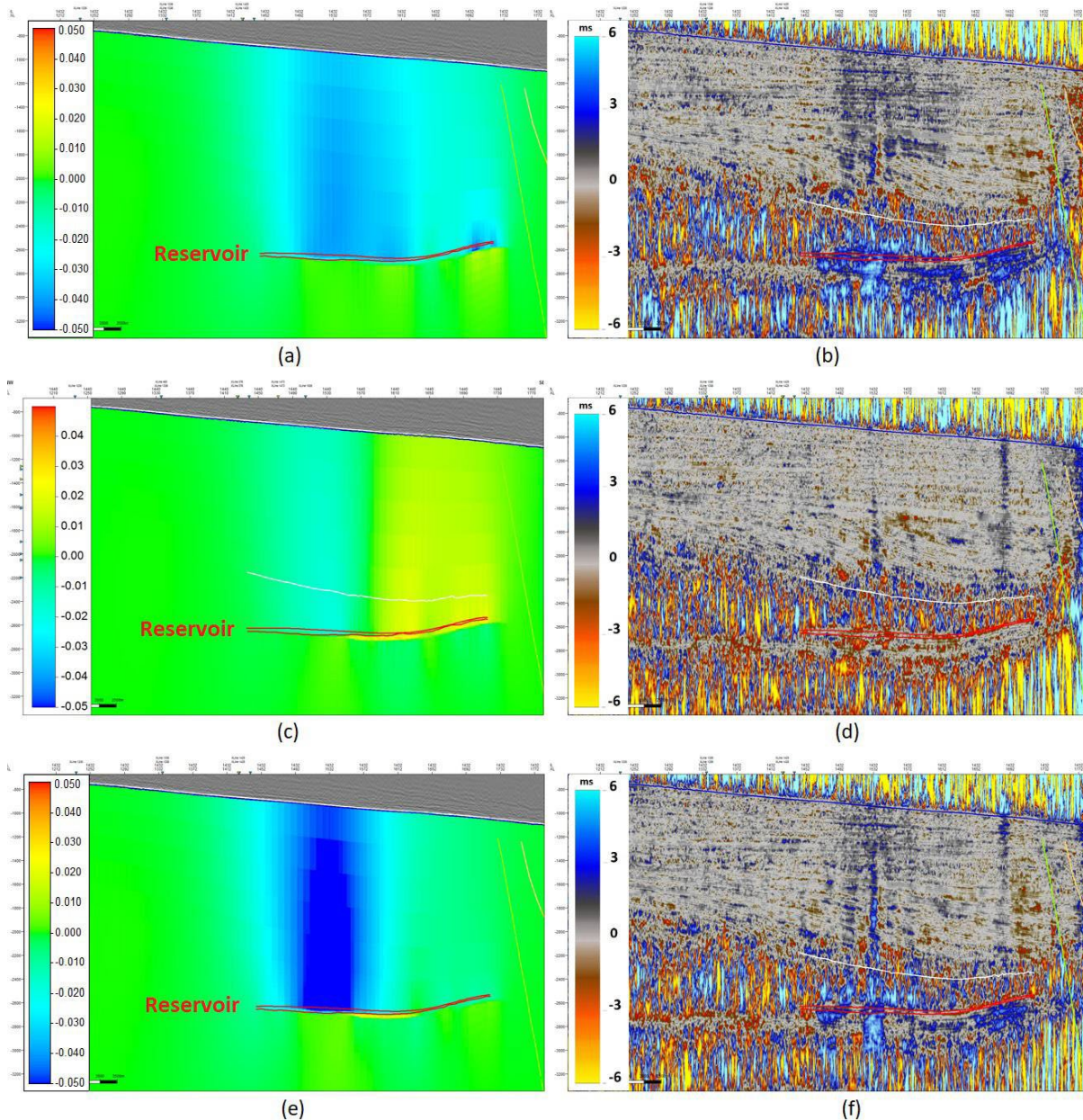Figure 7: Location of sections in the area of interest. Dip (A, C, D) and strike (B, E).

Figure 8: Section A – (a) the simulated displacement between 1997 and 2005, (b) the time shift calculated by the DTW technique between 1997 and 2005, (c) the simulated displacement between 2005 and 2010, (d) the time shift calculated by the DTW technique between 2005 and 2010, (e) the simulated displacement between 1997 and 2010, and (f) the time shift calculated by the DTW technique between 1997 and 2010.

anomalies. This can be seen in the period between 2005 and 2010, when the anomaly in yellow of the geomechanical uplift is not detected by the time shift on its right, in contrast to the slight depletion to its left that is discreetly perceived. Among the major anomalies of overpressure, in the period between 2005 and 2010, it appears a velocity fall anomaly that extends from the sea floor and goes towards the reservoir.

This anomaly is not expected and it was not possible to correlate it with anything other than a possible noise, despite its characteristic fingerprint,

present as a characteristic form of signal. Figure 9 is again section A with time shifts calculated by the cross-correlation technique. It reaffirms the observations made in the given DTW, showing very similar spatially and slightly shifted responses to depth, but without harming the interpretations, taking the analyzes to the same conclusions.

The strike section B cuts the dip section A in order to observe the anomalies more completely. The blank bands are regions where there was a lack of coverage in at least some of the data used in the 4D processing,
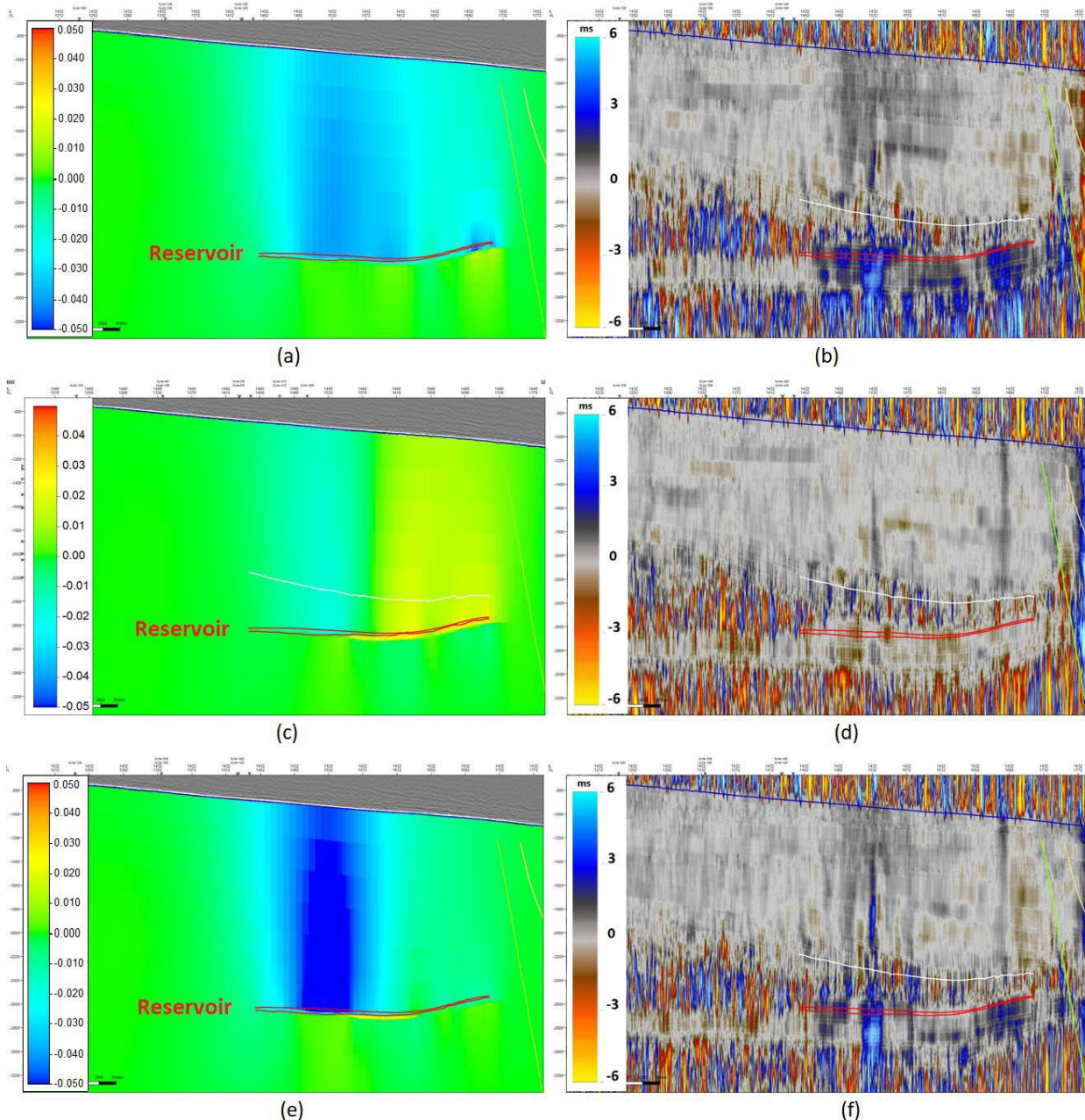
Figure 9: Section A – (a) the simulated displacement between 1997 and 2005, (b) the time shift calculated by the cross-correlation technique between 1997 and 2005, (c) the simulated displacement between 2005 and 2010, (d) the time shift calculated by the cross-correlation technique between 2005 and 2010, (e) the simulated displacement between 1997 and 2010, and (f) the time shift calculated by the cross-correlation technique between 1997 and 2010.

which preclude a safe analysis and should be disregarded. In Figure 10, it is possible to perceive the depletion anomalies in blue, in both geomechanics and time shifts.

However, in the latter, the data seem to present alternating vertical signal bands with no signal bands, showing that the data may be influenced by the unresolved noise during the 4D seismic processing step. This eventually hinders interpretation, but time shifts can be observed and indicate regions where there are

geomechanical effects caused by production effects. Again, between 1997 and 2005, the signal is more intense, with little sign between 2005 and 2010, reappearing with intensity between 1997 and 2010, confirming the expectations of the pressure data and also, to a great extent, of the geomechanical simulation.

Near the central region of the time-shift anomaly, there is a feature similar to a geological fault. Making a survey by the amplitude data and structural attributes, it is possible to perceive that there is a
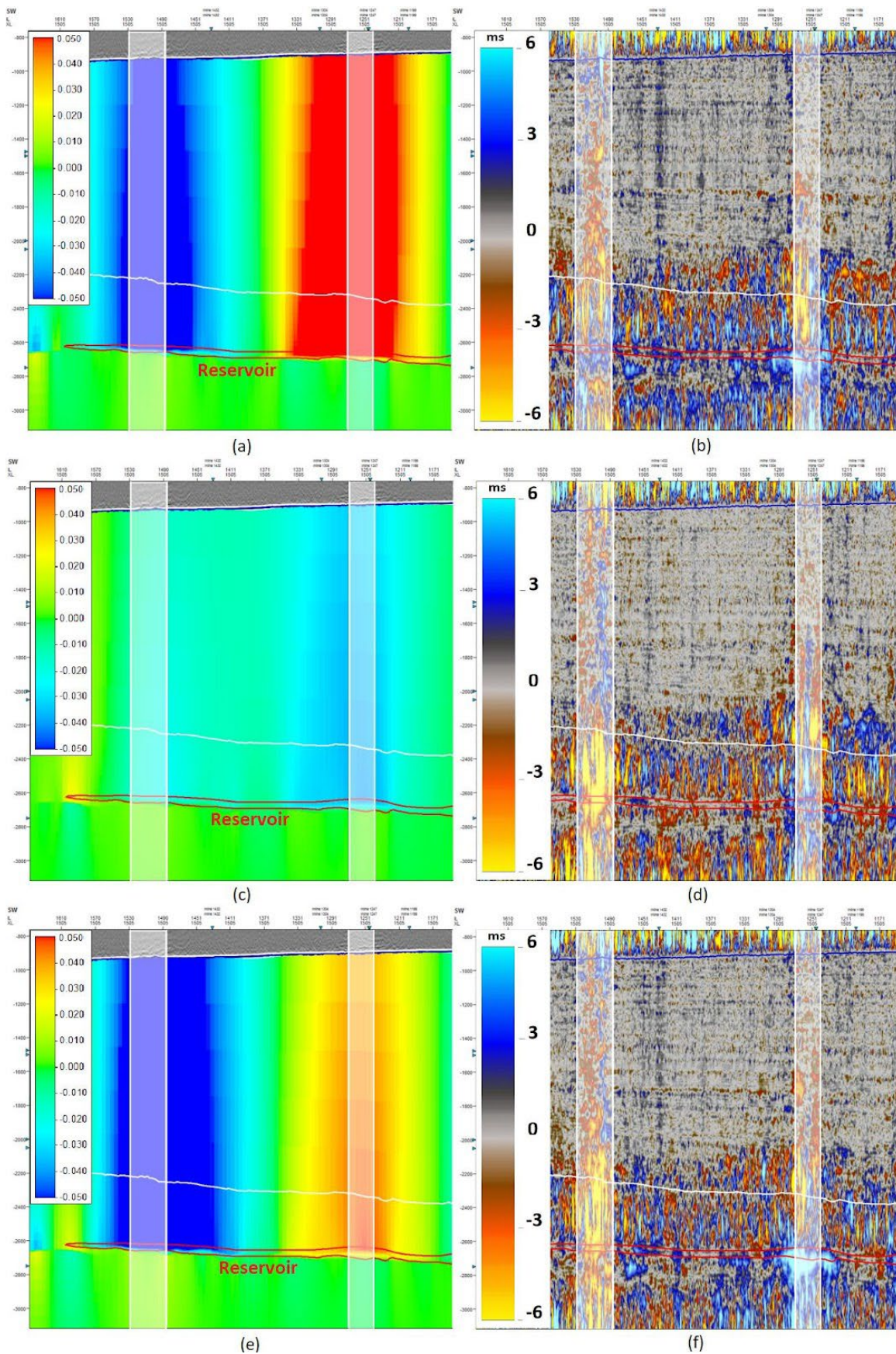
Figure 10: Section B − (b) the time shift calculated by the DTW technique between 1997 and 2005, (c) the simulated displacement between 2005 and 2010, (d) the time shift calculated by the DTW technique between 2005 and 2010, (e) the simulated displacement between 1997 and 2010, and (f) the time shift calculated by the DTW technique between 1997 and 2010.

discontinuity little perceived in the amplitude data, but this indicates a sub-seismic fault in the structural attribute of variance. The feature is indicated by red arrows in [Figure 11](#). With data indications and structure agreement with major field faults, this feature is likely to be a hard-to-detect subsurface fault and is highlighted by the time-shift data. In the position of the feature in the given period from 1997 to 2005 ([Figure 11](#)), there is a strong anomaly in blue indicating a decrease in velocity next to a strong anomaly in red indicating an increase of velocity. With the possibility of a sub-seismic fault, it is acceptable to assume that the pressure drop of the reservoir may have caused an accumulation of tensions in the region causing these variations in the seismic velocities. Nevertheless, this information does not appear in the geomechanical model and can be added in a future update, increasing its predictability and confidence in the simulations.

Another important point is the possibility that this region of the sub-seismic fault is serving as a migration path for reservoir fluids to rise to overburden permoporous layers. This region of the reservoir has a gas cap due to the pressure drop, and it is known that a small concentration of gas in the rock can considerably reduce the seismic velocity; therefore, it is likely that light hydrocarbons may be taking advantage of these ducts. It is difficult to say whether subsistence faults already existed before field production began, or whether they may be being stimulated by production, but it is known that these structures are present in time shift and require attention from the reservoir management.

In the central region of the field, where the largest overpressure anomaly of the period from 1997 to 2010 exists, there is the dip section C. Here, the excess pressure anomalies are difficult to detect. The highest intensity of the simulated uplift is between 1997 and 2005 and it can be seen in [Figure 12](#).

There are practically no 4D anomalies in the region; just to the upper right corner, between the 2005 and 2010 period, it appears a positive anomaly in strong blue which can be explained by a part of the field operation that has been moved to another region. An anomaly of this type hardly represents any effect on the rocks of the overburden because they are not consistent up to the reservoir. This possibility, which can interfere in the analysis of section C, considering that before the overpressure in this period there was a pressure drop, may have caused the effect of the hysteresis, causing the overburden tension not to return to the previous state in the same way that occurred in the process of depletion

and relief of the rocks, complicating the recovery process of the stress, a movement that would increase the propagation velocity of the seismic wave. In this region, there was no significant anomaly on the part of 4D seismic, making it difficult to get a comparison and any other assertion about the predictability of the geomechanical simulations.

The dip D section is located in the northern region of the field where, similarly to the southern region, it is expected the overburden rocks to dilate, since in this region the time shift does not confirm the predictions of the geomechanics. In [Figure 13](#), we can observe a simulated geomechanical anomaly that between 1997 and 2005 shows a subsidence of the seafloor followed by similar displacements by almost all extension above the reservoir, showing good symmetry between the pressure drop and the compaction effects of the reservoir. The time shift shows a high-intensity anomaly indicating a velocity drop near the field boundary faults, in a region well structured by extension faults that are associated with halokinetic movements that extend close to the seabed.

Thus, there is no agreement between the results. Knowing that the geomechanical model gathers information from many modeling and interpretation processes, in addition to not using the faults for the simulation process, and that the time-shift data are practically a measure without many previous processes, it is plausible to treat the 4D seismic results as more reliable. This information is of extreme importance for a future update of the geomechanical model, for new predictions about the stability of the transmissibility of these faults and also on the impact on field pressure adjustment, since the pressure information is one of the main inputs of the geomechanical modeling.

In order to support the greatest reliability in the time-shift data, the structural attributes were analyzed. Between 2005 and 2010, the disagreement is similar, the results are still not discussed, and an unexpected anomaly occurs. Where there was a strong time-shift anomaly between 1997 and 2005, an anomaly of increase in seismic velocities appears; something difficult to detect, indicating that there was a geomechanical deformation of sufficient intensity to change the field of tensions to the point of being detected by the 4D seismic, showing once again that the aforementioned structured region suffers more intensely the pressure variations occurring in the reservoir. At the center of section D and to the left of the seismic velocity anomaly, it is possible to notice in the time-shift data that a pressure drop anomaly is
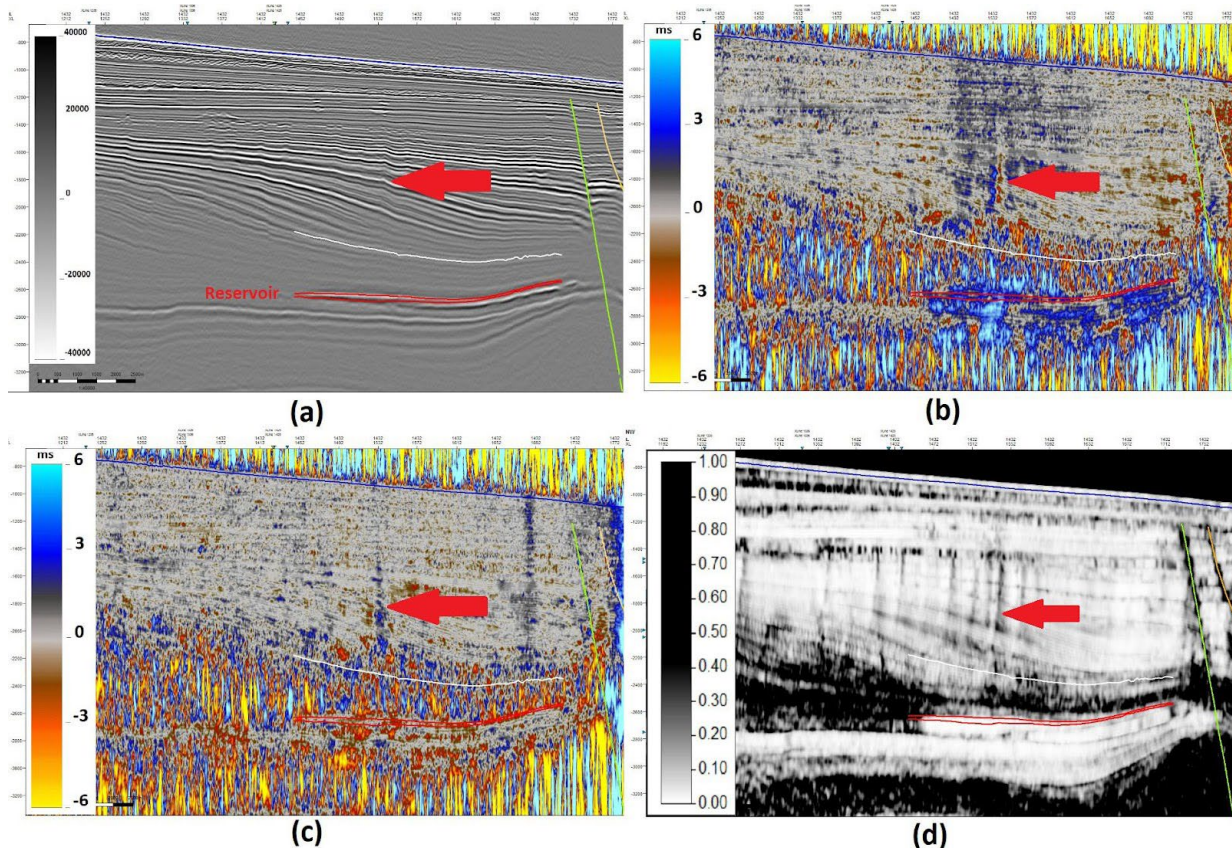
Figure 11: Section A with red arrows indicating the structural feature, taking (a) the 1997 3D seismic data, (b) the time shift calculated by the DTW technique between 2005 and 2010, (c) the time shift calculated by the DTW technique between 1997 and 2005, and (d) the structural variance attribute.

present. This confirms that the movements that occurred in the overburden in the northern region of the field were not well represented by the geomechanical modeling. Between 1997 and 2010, a slight depletion anomaly appears in the time-shift section, agreeing with the simulation.

The strike section E cuts the dip section D. The blank strips are regions where there is a lack of coverage. In the section it is possible to notice the strong structuring in the edge faults of the field. Analyzing Figure 14, it is possible to notice that the 4D time-shift anomaly between the dates 1997 and 2005 seen in the dip section of the same date has spatial consistency and concentrates again near the border extension faults, confirming the previous analysis. Between 2005 and 2010, the velocity increase anomaly is also consistent, reaffirming that the anomalies have a geometric distribution not consistent with noise.

## Structural pattern and Time shifts

The turbidic field studied in this paper has a strong influence of the salt tectonics, an assertion already introduced in the description section of the study area.

An example of how the 4D time shift can contribute to the understanding of field structures and their relationship to production effects is now presented. The field is structurally limited by extension border faults to the east and stratigraphically and structurally limited to the west. This structural evolution can be seen in the dip section in the south of the field (Figure 1), which shows the layout of the salt diapirs and the large extension faults. These faults seem to continue to occur with small displacement being less noticeable in 3D seismic. The structural feature mentioned in section A can be interpreted as one of those faults that are difficult to map in 3D data, but are highlighted in some structural attributes, such as variance. In order to better visualize these structures and to correlate them more clearly with the extension faults associated to halokinese, a depth-cut of the variance attribute is shown in Figure 15 with a red contour of the reservoir projection. These faults largely follow the north-south trend, as shown by the north-east extension faults. As the east approaches, the faults take the form of the extension structures associated with the southeast salt diapir. Even though it is more noticeable in the
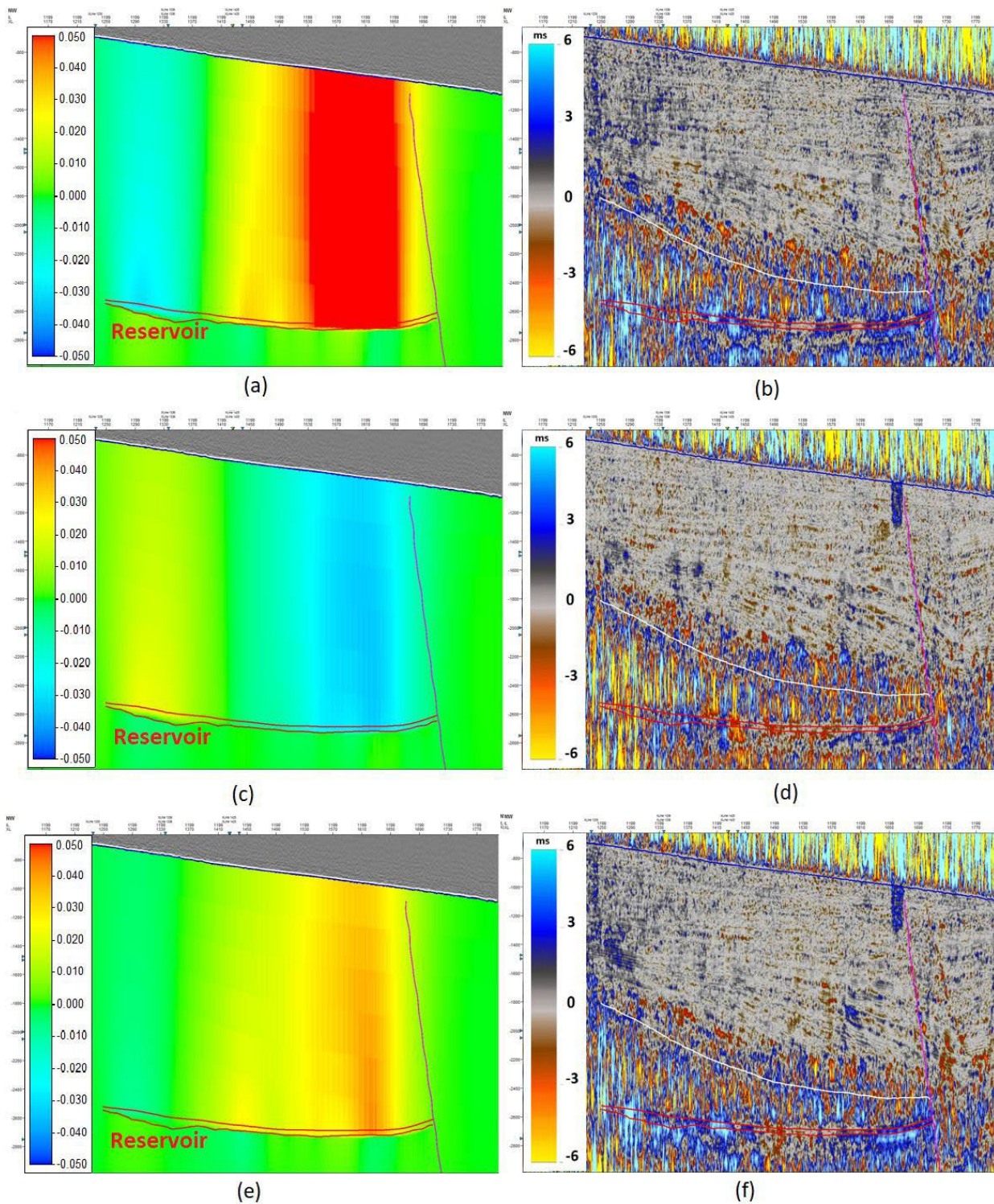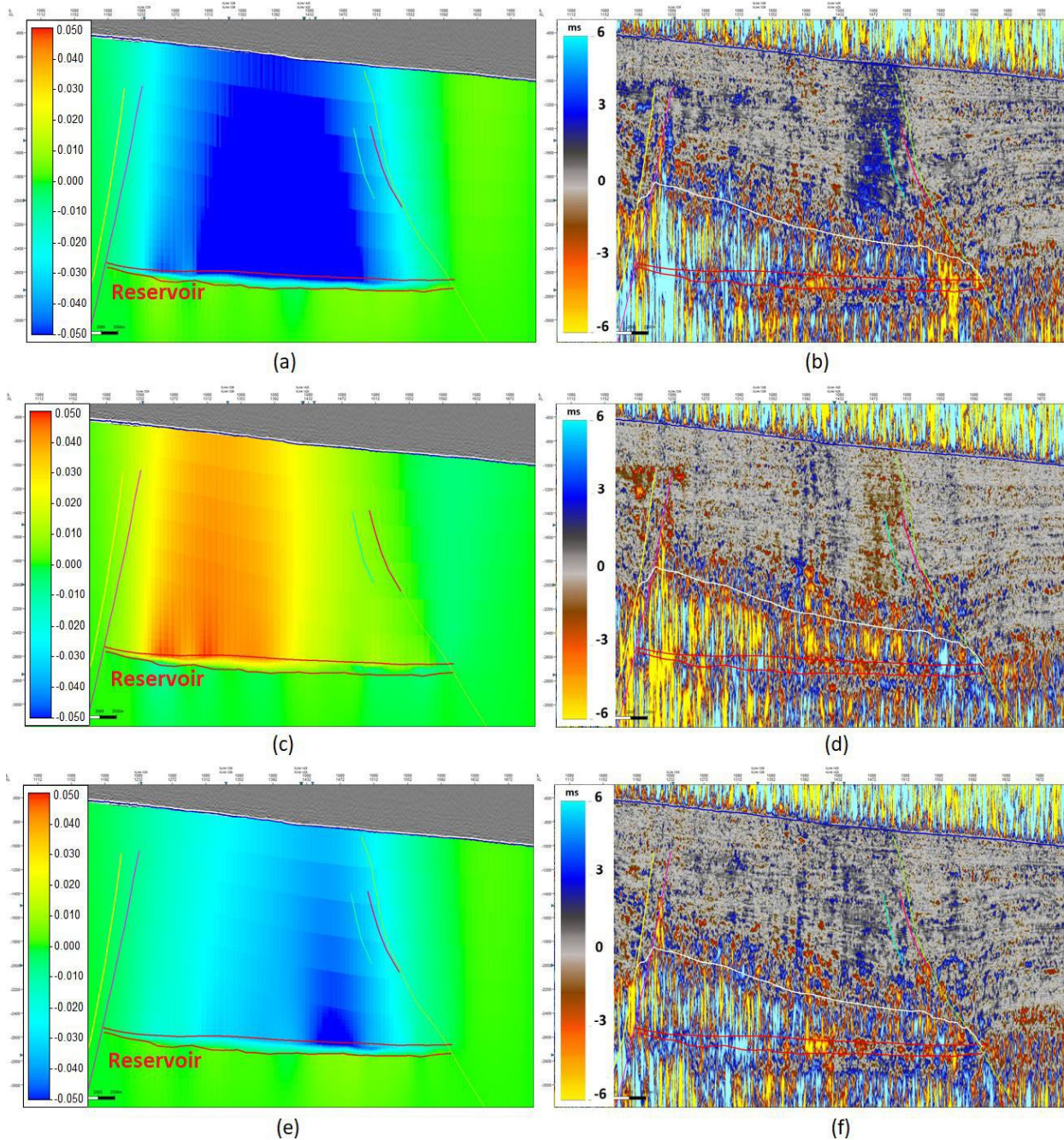
Figure 12: Section C − (a) the simulated displacement between 1997 and 2005, (b) the time shift calculated by the DTW technique between 1997 and 2005, (c) the simulated displacement between 2005 and 2010, (d) the time shift calculated by the DTW technique between 2005 and 2010, (e) the simulated displacement between 1997 and 2010, and (f) the time shift calculated by the DTW technique between 1997 and 2010.

structural attribute, the characteristic of these sub-seismic faults in the 3D data is only a slight change in the reflectors upwards, as a small mound, which is detected by the variance (Figure 16). These hills may be

associated with a drop in seismic velocity caused by the rise of fluids that take advantage of these ducts. As the velocity model does not represent these velocities, the reflectors end up overcorrected and pulled up.

Figure 13: Section D, where (a) is the simulated displacement between 1997 and 2005, (b) the time shift calculated by the DTW technique between 1997 and 2005, (c) the simulated displacement between 2005 and 2010, (d) the time shift calculated by the DTW technique between 2005 and 2010, (e) the simulated displacement between 1997 and 2010, and (f) the time shift calculated by the DTW technique between 1997 and 2010.

The objective of the more detailed analysis of these structures arises with the observation of some time-shift anomalies that coincide with their lineaments. Figure 17 shows an overburden region south of the field through a dip section and a depth cut of 1615 m. In the section, we can see the positive 4D time-shift anomaly indicating a drop in the seismic velocity practically embedded between two structures

of the sub-seismic fault type, structures that are highlighted by the variance in the depth cut. In red, we have a projection of the reservoir boundary, corroborating with factors related to the production effects that may have caused this anomaly in 4D seismic. This information leads us to see these structures as divisions between partially independent movable blocks of structure.
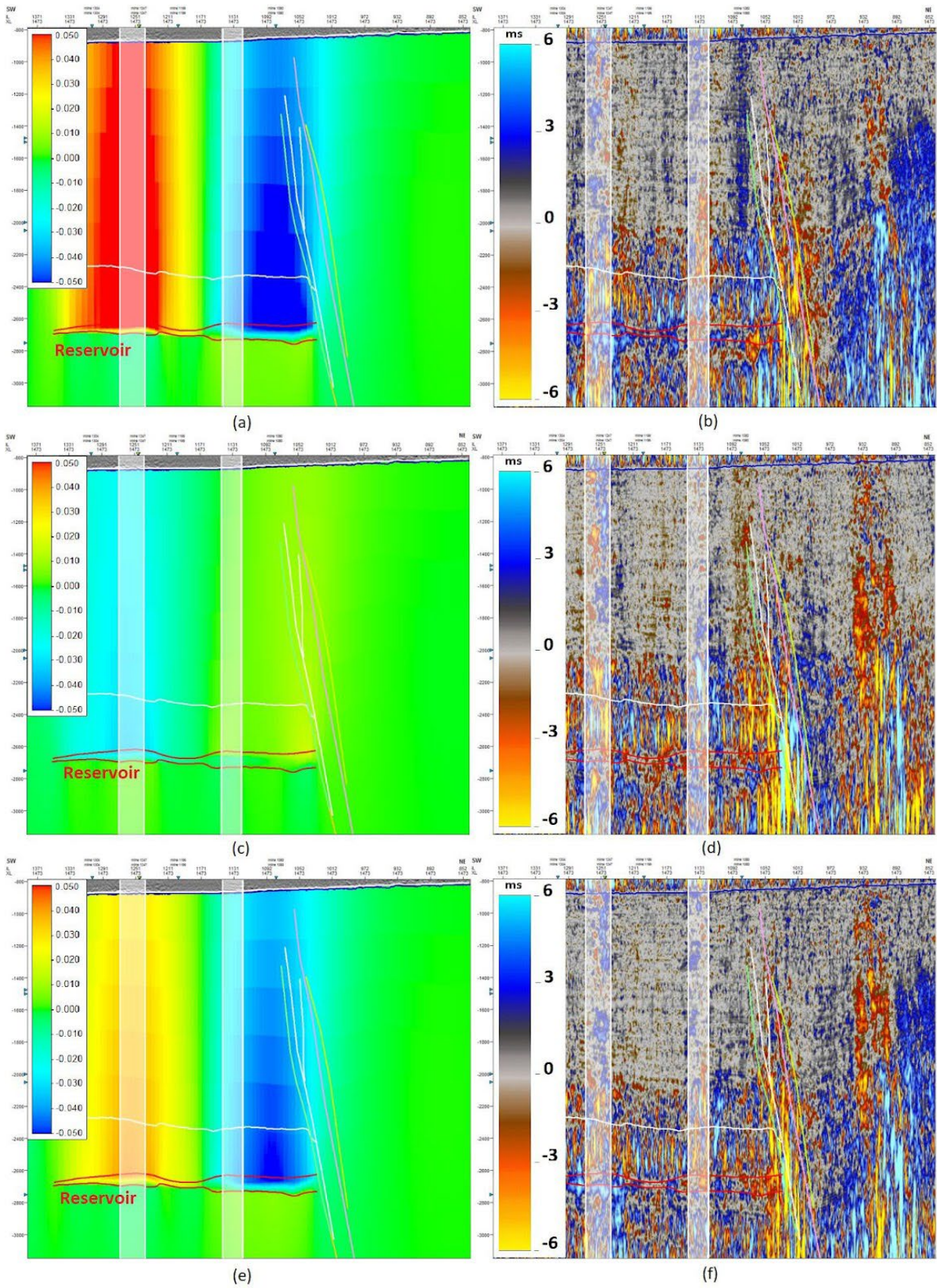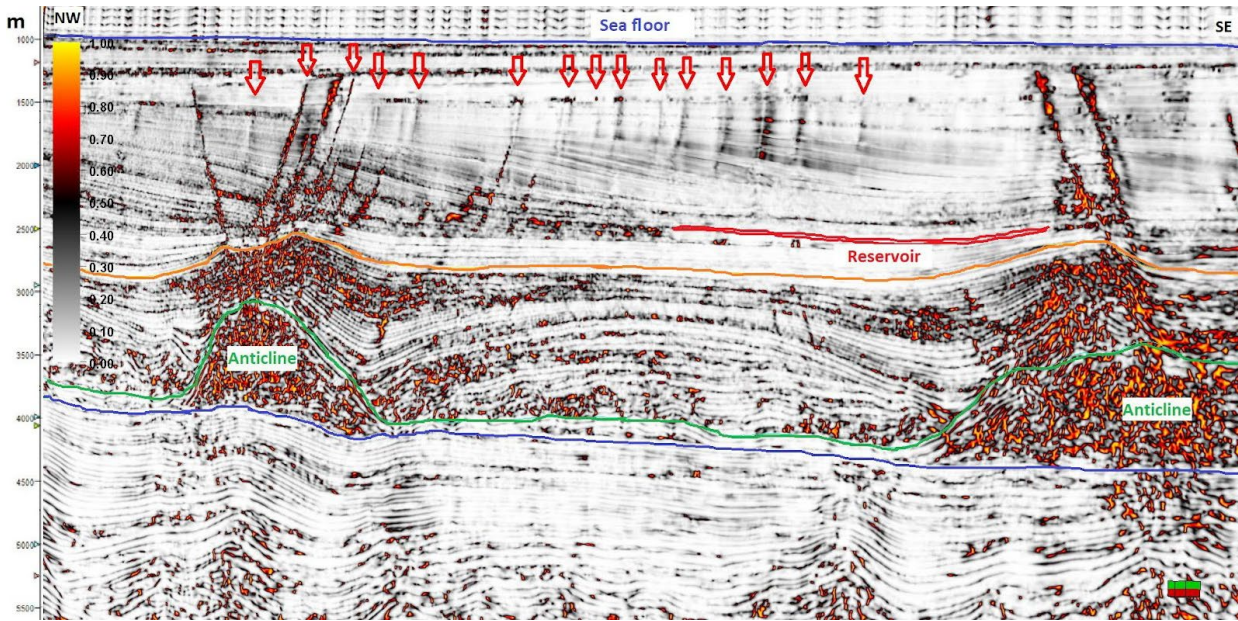
Figure 14: Section E − (b) the time shift calculated by the DTW technique between 1997 and 2005, (c) the simulated displacement between 2005 and 2010, (d) the time shift calculated by the DTW technique between 2005 and 2010, (e) the simulated displacement between 1997 and 2010, and (f) the time shift calculated by the DTW technique between 1997 and 2010.

Figure 15: Dip section of the southern region of the field with structural attribute of the variance. The arrows in red indicate structures associated with the extension movements.
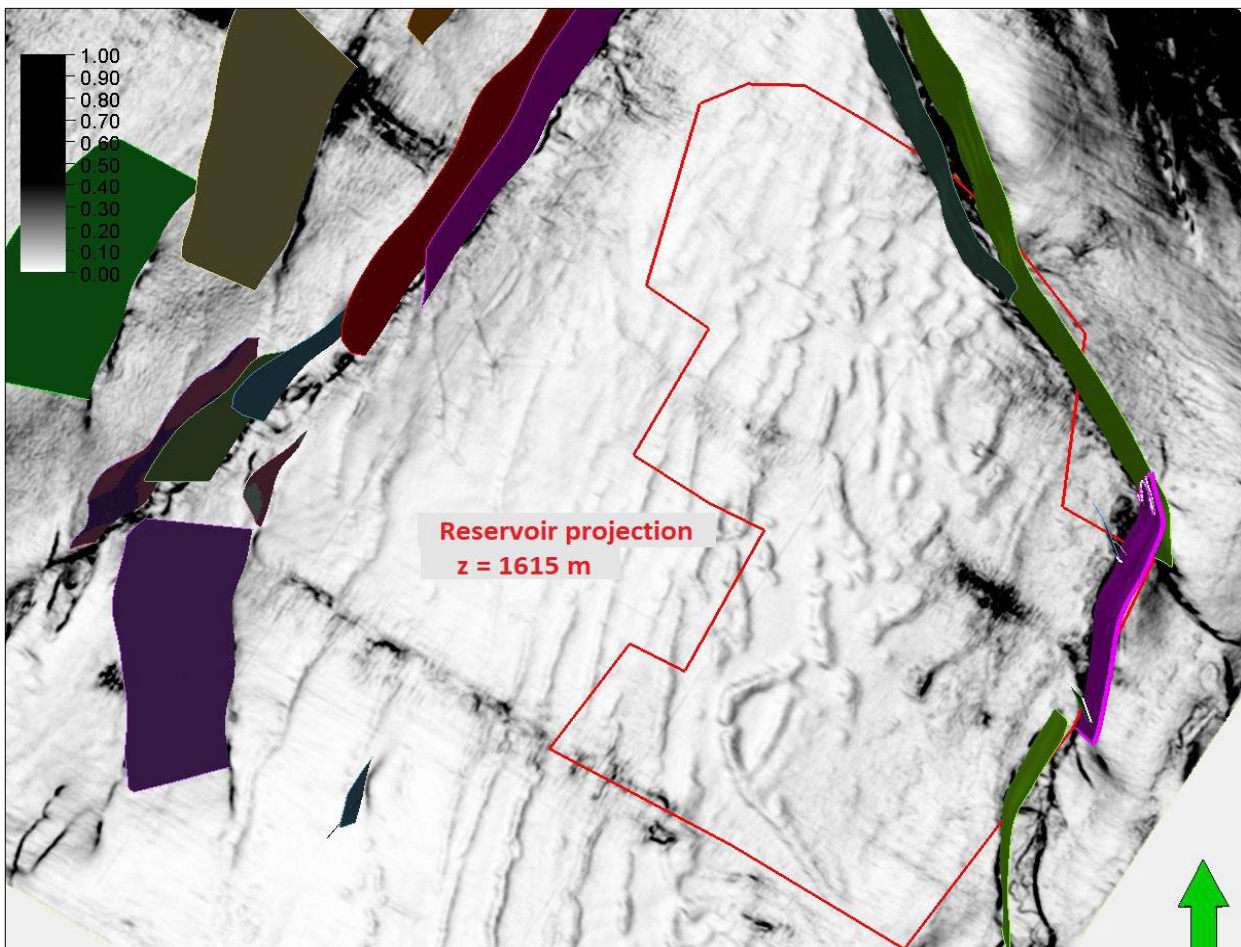


Figure 16: Variance attribute at the depth cut z = 1615m. We can see these structures as divisions between partially independent movable blocks of structure.

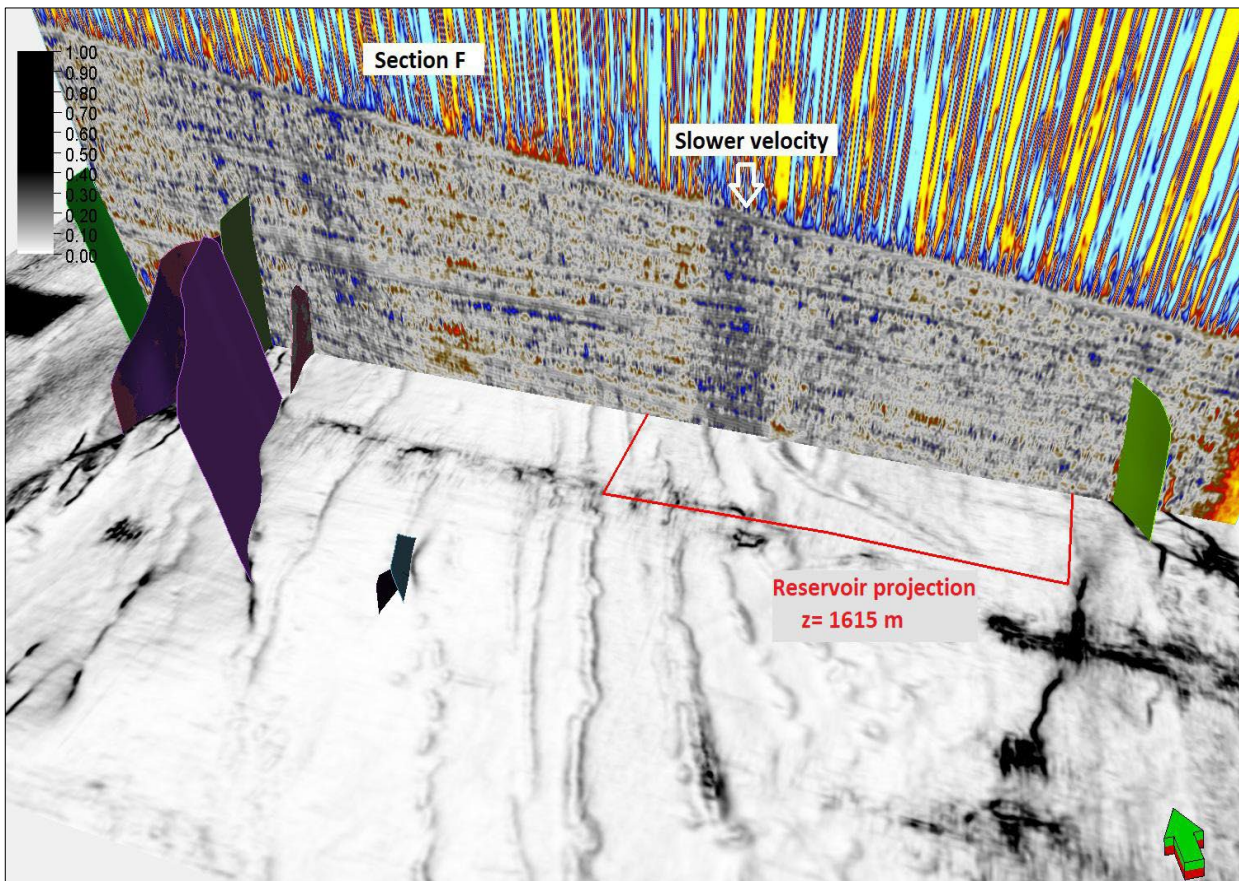Figure 17: Time-shift anomaly in a section (dip) and the variance attribute at the depth cut z = 1615m.

Consequently, it shows how time shifts can influence the understanding of the field structure and decision making of reservoir management. Better understanding and tracking of these structures are of outmost importance for the safety of operations.

The geomechanical simulation indicates in the same area a dilation of the geomechanical rocks, confirming what is observed in the 4D seismic. However, the simulation shows a distribution of the dilated anomaly well smoothed and laterally continuous. In Figure 18 you can see these characteristics. This, once again, shows the value of the 4D information since the detail about the structures is hardly mapped in the 3D seismic and without this information it is difficult to represent this detail in the geomechanical modeling. Figure 19 shows the time-shift anomaly with the projection of the pressure anomaly in the reservoir, noting the coherence among the data, differing only in the fact that the block in which the 4D anomaly appears affected more the compaction of the reservoir than the neighbour blocks. As the pressure map and the contour of the reservoir are a projection, it must be considered that the anomaly is somewhat displaced from the original position that touches the reservoir, since we

have seen that the sub-seismic faults appear sub vertical, with some inclination.

## DISCUSSION

A robust estimate of the R factor depends mainly on a reliable time-shift anomaly consistent with the production, in addition to a predicted forecast of the geomechanical simulation. In a previous section, a value of R was found through a statistical estimate of 1300. This value shows the high sensitivity of the overburden of the area studied in this paper. This indicates that small geomechanical deformations cause variations in seismic velocities sufficient to be detected. As the R Factor is layer-dependent (MacBeth et al., 2018), the closer to the seafloor, the R-values tend to be larger (Røste et al., 2015). R = 1300 means a high sensitivity of the overburden in relation to the geomechanical deformation, what made it possible to perceive time-shift anomalies consistent with the production effects.

Starting from the result of the more reliable R-value, it was possible to construct synthetic 4D time shifts closer to the real ones. Figure 20 shows the synthetic 4D time shift calculated from the R Factor =
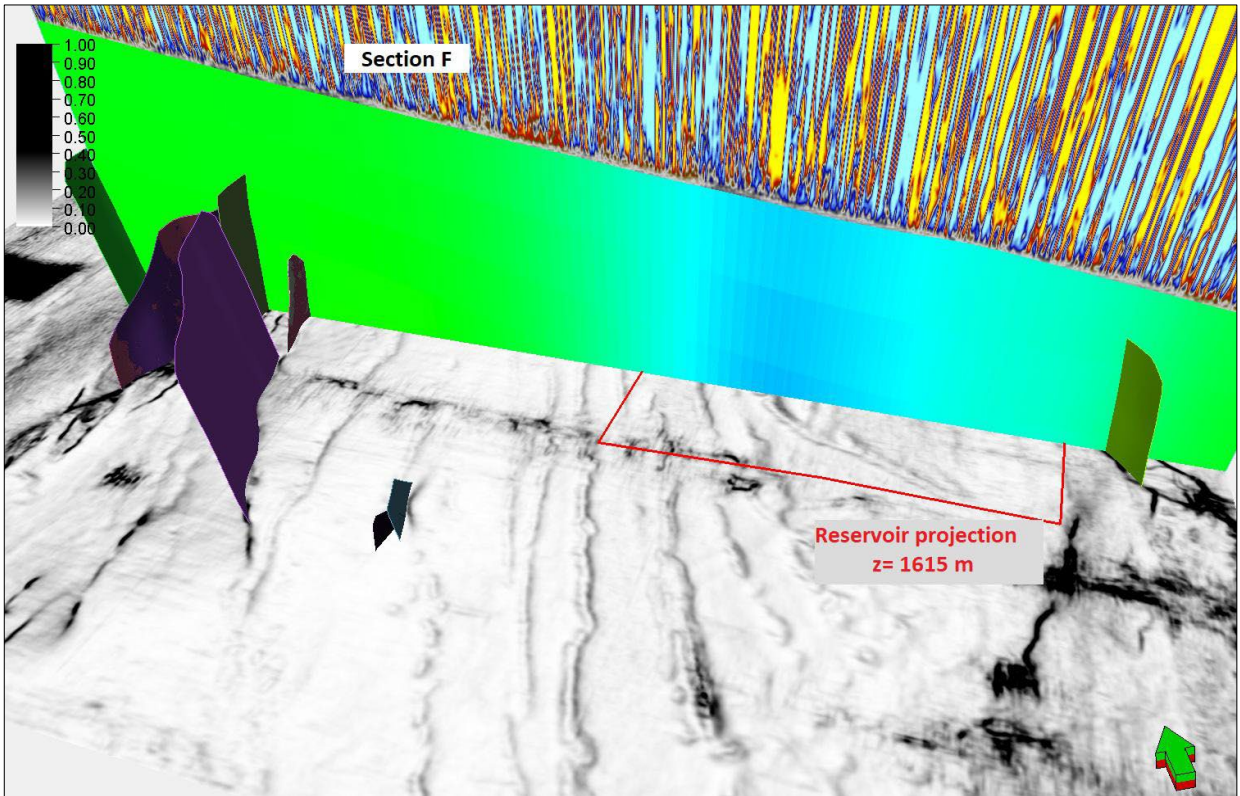
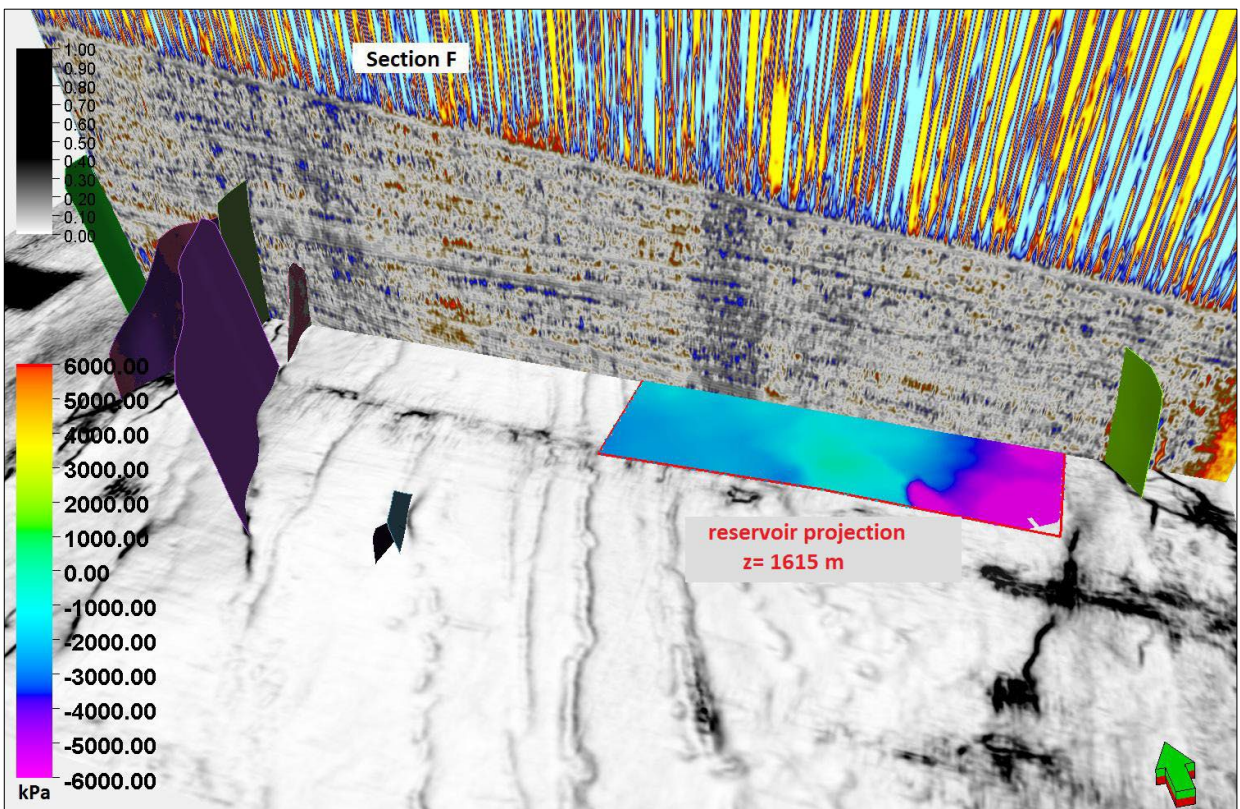Figure 18: Section (dip) with geomechanical displacements with structural attribute of the variance at z = 1615m.



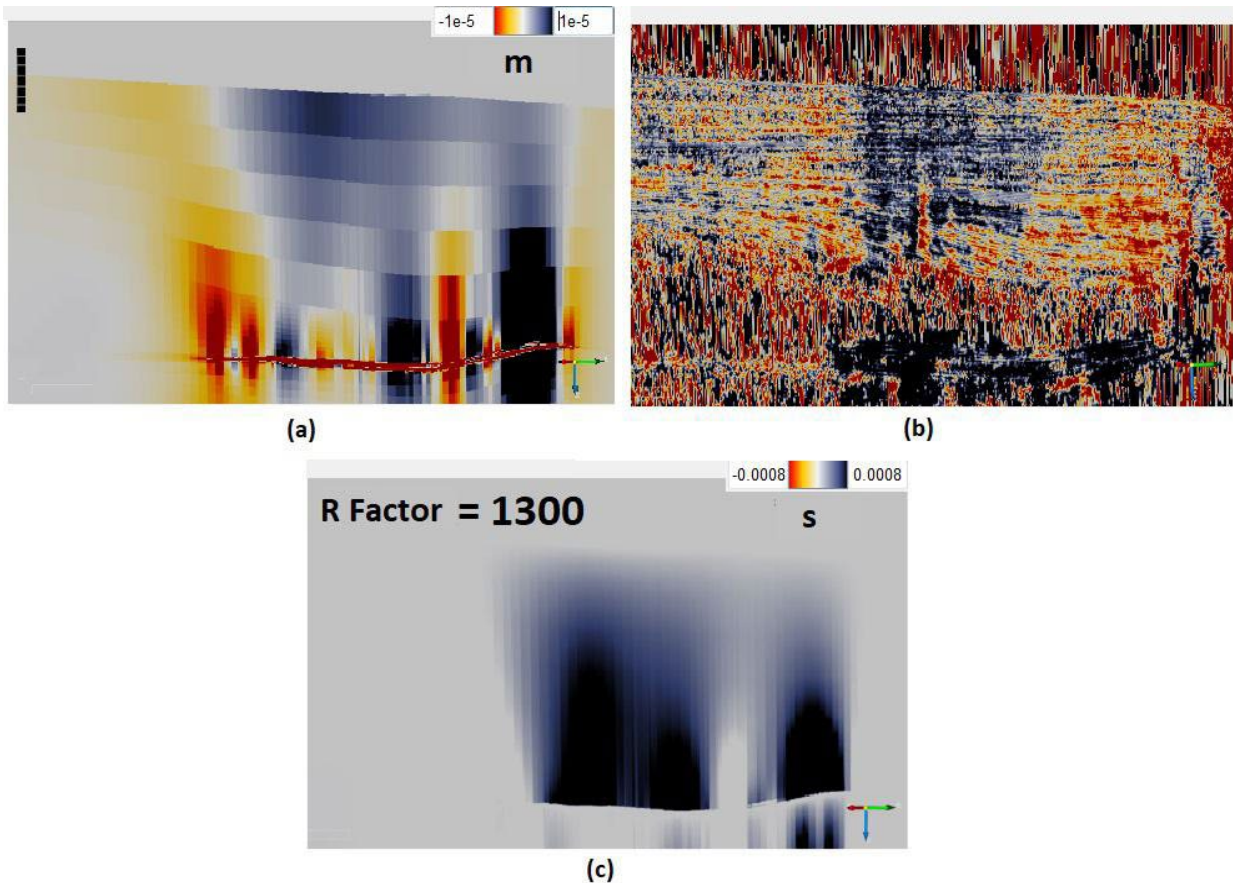Figure 19: Time-shift section (dip) with pressure variation in the designed reservoir at z = 1615m.

Figure 20: Section A − (a) deformation, (b) real 4D time shift, (c) synthetic 4D time shift with R = 1300.

1300 and the strain matrix, zz. Other values of R can be calculated. The R Factor is dependent on the lithology and the initial state of stress; therefore, in several overburden intervals, different values can be extracted which will represent the estimated region better than the others. An approximate R-value for the field is of great importance for the predictability of geomechanical deformations in a future interpretation of 4D time-shift data, either reprocessed data or a new 4D seismic acquisition.

Other physical processes not reported in detail in this paper may cause 4D time shifts. Among them there are reasons that can cause real anomalies, such as reactivation of faults, injection outside the reservoir zone and hydrocarbon leaks. A distinct possibility is that of noise produced during the acquisition and processing of seismic data, processes that may cause artificial anomalies. The time shifts analyzed in this paper are in regions of good quality and low noise levels; even in regions of faults, the levels remained low. The anomalies agree with the field pressure data, being consistent with the production, and can hardly be related to other effects.

## CONCLUSION

It was possible to extract important information for field management from 4D time shifts in the overburden region of the Campos Basin turbiditic reservoir. Even without large pressure variations between the studied periods and maximum variations in the seafloor close to 5 cm, it was possible to detect the effect of geomechanical changes through the variations of seismic velocities in regions of the field where there was mainly depletion. For the analyzes to be done with better security, an adjusted model of field pressure is required, a geomechanical model with as much information as possible and, not least, well processed 4D seismic.

When comparing geomechanical shifts and time shifts, it was possible to evaluate how close the simulation forecasts are to those of the 4D data. Among the depletion regions, the southern region of the field presents a correlation between the methodologies, but in the northern region there was no similar agreement, attributed mainly to the region heavily structured by extension faults associated with the tectonics. From this interaction, it was possible to generate information

capable of being used in an update of both the field pressure adjustment and the geomechanical simulation model, showing the importance of using geological faults in the simulations to increase the predictability of the deformations. In most regions where there were strong overpressure effects, time shifts were not able to detect significant variations in seismic velocities, confirming what has been found in other published papers on the subject, and associating this phenomenon with the effects of hysteresis. The only exception came from the data between 2005 and 2010, when an anomaly was found responding with a slight increase in velocities due to overpressure.

A direct relationship between seismic velocity variations and the vertical strain tensor proved to be inefficient in selecting an R factor that could be used in the construction of synthetic time shifts. However, a statistical form of estimation was proposed and presented a satisfactory result, indicating the value of R equal to 1300 for a region where the 4D anomalies fit well with the geomechanical simulations. This value is much greater than the values found in the North Sea Chalk fields, which confirms the expected possibility and shows that, in the region studied in this paper, the overburden is much more sensitive in relation to variations of seismic velocities caused by geomechanical deformations than in other places with large deformations in the rocks above the reservoir. For this reason, anomalies can be detected and interpreted, bringing useful information to the understanding of the field. With the result of the more reliable R-value, it was possible to construct synthetic 4D time shifts closer to the real ones, increasing the predictability of finding geomechanical deformations in a future time-shift interpretation in a new 4D seismic acquisition.

Thus, this paper highlights the possibility of adding valuable information to reservoir management through 4D seismic time shifts. The relationship between the 4D data and the geomechanical and structural aspects of the field contributes to the estimation of geomechanical variations directly from 4D seismic and indicates areas of the reservoir that are more compact with the effects of production.

## ACKNOWLEDGMENTS

## REFERENCES

Barkved O., P. Heavey, R. Kjelstadli, T. Kleppan, and T.G. Kristiansen, 2003, Valhall field - still on plateau after 20 years of production: SPE Offshore Europe Oil and Gas Exhibition and Conference, Society of Petroleum Engineers, Aberdeen, United Kingdom, Paper 83957, doi: 10.2118/83957-MS.

Demercian, S., P. Szatmari, and P.R. Cobbold, 1993, Style and pattern of salt diapirs due to thin-skinned gravitational gliding, Campos and Santos basins, offshore Brazil: Tectonophysics, **228**, 393–433, doi: 10.1016/0040-1951(93)90351-J.

Dusseault, M.B., 2007, CHOPS: Cold Heavy Oil Production with Sand, *in* Warner Jr., H.R., ed., Petroleum Engineering Handbook: Emerging and Peripheral Technologies (EMPT), SPE, volume VI, chapter 5, p. 40.

Fiore, J., C. Hubans, and E. Brechet, 2014, 4D Seismic Warping in Two Steps for Overburden and Reservoir - Example of a Compacting Carbonate Field: 76th EAGE Conference and Exhibition, New Orleans, Louisiana, USA, doi: 10.3997/2214-4609.20140763.

Garcia, A., and C. MacBeth, 2013, An estimation method for effective stress changes in a reservoir from 4D seismics data: Geophysical Prospecting, **61**, 4, 803–816, doi: 10.1111/1365-2478.12035.

Hale, D., 2013, Dynamic warping of seismic images: Geophysics, **78**, 2, S105–S115, doi: 10.1190/geo2012-0327.1.

Hatchell, P., and S. Bourne, 2005a, Measuring reservoir compaction using time-lapse timeshifts: 75th Annual International Meeting, SEG Technical Program Expanded Abstracts, Houston, Texas, USA, 2500–2503, doi: 10.1190/1.2148230.

Hatchell, P., and S. Bourne, 2005b, Rocks under strain: strain-induced time-lapse time shifts are observed for depleting reservoirs: The Leading Edge, 24, 1222–1225, doi: 10.1190/1.2149624.

Herwanger, J., E. Palmer, and C.R. Schiøtt, 2007, Anisotropic velocity changes in seismic time-lapse data: 77th Annual International Meeting, SEG, Expanded Abstracts, 2883–2887, doi: 10.1190/1.2793065.

Landrø, M., 2001, Discrimination between pressure and fluid saturation changes from time-lapse seismic data: Geophysics, **66**, 836–844, doi: 10.1190/1.1444973.

Landrø, M., and J. Stammeijer, 2004, Quantitative estimation of compaction and velocity changes using 4D impedance and traveltime changes: Geophysics, **69**, 4, 949–957, doi: 10.1190/1.1778238.

Macbeth C., A. Kudarova, and P. Hatchell, 2018, A semi-empirical model of strain sensitivity for 4D seismic interpretation: Geophysical Prospecting, **66**, 7, 1327–1348, doi: 10.1111/1365-2478.12648.

Mohriak, W.U., D.E. Brown, and G. Tari, 2008, Sedimentary Basins in the Central and South Atlantic Conjugate Margins: Deep Structures and Salt Tectonics, *in* Brown, D.E. and N. Watson, eds., Extended Abstracts: Central Atlantic Conjugate Margins Conference, Halifax, Nova Scotia, Canada, CD, 89–102.

Røste, T., A. Stovas, and M. Landrø, 2005, Estimation of layer thickness and velocity changes using 4D prestack seismic data: 67th EAGE Conference and Exhibition, Madrid, Spain, doi: 10.3997/2214-4609-pdb.1.C010.

Røste, T., O.P Dybvik. and O.K. Søreide, 2015, Overburden 4D time shifts induced by reservoir compaction at Snorre field: The Leading Edge, **34**, 1366–1374, doi: 10.1190/tle34111366.1.

Røste, T., and G. Ke, 2017, Overburden 4D time shifts – Indicating undrained areas and fault transmissibility in the reservoir: The Leading Edge, **36**, 423–430, doi: 10.1190/tle36050423.1.

Wong, M.Y., and C. MacBeth, 2016, R-factor Recovery via Geertsma's Pressure Inversion Assisted by Engineering Concepts: 78th EAGE Conference and Exhibition, European Association of Geoscientists & Engineers, Vienna, Austria, WS14 B02, doi: 10.3997/2214-4609.201601670.

Zoback, M.D., and J.C. Zinke, 2002, Production-induced normal faulting in the Valhall and Ekofisk oil fields: Pure and Applied Geophysics, **159**, 403–420, doi: 10.1007/PL00001258.

**Cardoso, C.A.R.:** preparation, creation, revision; **Moraes, F.S.:** time-shift calculation support, article review; **Lima, K.T.P.:** support for the understanding of the structural geology of the area.